The Journal of Experimental Biology 214, 3386-3395

doi:10.1242/jeb.050252

RESEARCH ARTICLE

Differential segmental strain during active lengthening in a large biarticular thigh muscle during running

Jennifer A. Carr*,†, David J. Ellerby‡ and Richard L. Marsh

Department of Biology, Northeastern University, Boston, MA 02115, USA

*Author for correspondence (carr@fas.harvard.edu)

†Present address: Department of Organismal and Evolutionary Biology, Harvard University, 26 Oxford Street, Cambridge, MA 02138, USA

‡Present address: Department of Biological Sciences, Wellesley College, 106 Central Street, Wellesley, MA 02481, USA

Accepted 24 May 2011

SUMMARY

The iliotibialis lateralis pars postacetabularis (ILPO) is the largest muscle in the hindlimb of the guinea fowl and is thought to play an important role during the stance phase of running, both absorbing and producing work. Using sonomicrometry and electromyography, we examined whether the ILPO experiences differential strain between proximal, central and distal portions of the posterior fascicles. When the ILPO is being lengthened while active, the distal portion was found to lengthen significantly more than either the proximal or central portions of the muscle. Our data support the hypothesis that the distal segment lengthened farther and faster because it began activity at shorter sarcomere lengths on the ascending limb of the length–tension curve. Probably because of the self-stabilizing effects of operating on the ascending limb of the length–tension curve, all segments reached the end of lengthening and started shortening at the same sarcomere length. During shortening, this similarity in sarcomere length among the segments was maintained, as predicted from force–velocity effects, and shortening strain was similar in all segments. The differential active strain during active lengthening is thus ultimately determined by differences in strain during the passive portion of the cycle. The sarcomere lengths of all segments of the fascicles were similar at the end of active shortening, but after the passive portion of the cycle the distal segment was shorter. Differential strain in the segments during the passive portion of the cycle may be caused by differential joint excursions at the knee and hip acting on the ends of the muscle and being transmitted differentially by the passive visco-elastic properties of the muscle. Alternatively, the differential passive strain could be due to the action of active or passive muscles in the thigh that transmit force to the IPLO in shear. Based on basic sarcomere dynamics we predict that differential strain is more likely to occur in muscles undergoing active lengthening at the beginning of contraction than those undergoing only shortening.

Key words: animal locomotion, differential strain, muscle physiology.

INTRODUCTION

Determining the mechanical function of large locomotor muscles is challenging because these muscles may have regional variation in function because of differences in morphology and/or motor recruitment (Chanaud et al., 1991; Lieberman et al., 2006; McGowan et al., 2006; Osternig et al., 1995). For example, fascicle strain, measured using sonomicrometry, combined with measures of electromyographic (EMG) activity reveals important information about the mechanical function of active muscles *in vivo*, but we lack enough information to predict the overall function of the large muscles from these local measures. This study and two companion studies (Carr et al., 2011a; Carr et al., 2011b) examine regional differences in function and overall mechanical function in the largest thigh muscle found in avian runners, the iliotibialis lateralis pars postacetabularis (ILPO).

The function of the ILPO in running birds is of particular interest because of the large size of the muscle, its high energy use and the association with the evolution of effective terrestrial locomotion by running. In birds that commonly run, the ILPO covers the posterior surface of the thigh and has extensor actions at both the hip and the knee. The muscle appears to be particularly large in birds adapted for running. For example, in our study species, the helmeted guinea fowl [*Numida meleagris* (Linnaeus 1758)], the ILPO is the largest single muscle in the hindlimb and demonstrates a disproportionate increase in blood flow between walking and running, indicating that it plays an important mechanical role during the stance phase of running (Ellerby et al., 2005; Marsh et al., 2004). By contrast, the ILPO is reduced or absent in birds with limited running abilities (Carr et al., 2011b).

The function of the ILPO during level, uphill and downhill running has been examined in two studies in guinea fowl (Buchanan, 1999; McGowan et al., 2006) and one study in turkeys (Roberts et al., 2007). The strain cycle documented in these studies suggests that this muscle acts as a brake in early stance, being lengthened while active, and a motor in late stance, shortening and producing work. These previous studies measured the strain of the ILPO in one fascicle segment at a single location in the muscle. Deducing the overall function from these data therefore requires the assumption that the strain cycle is uniform across the muscle. However, differential strain could occur along the axis from origin to insertion, particularly in the long posterior fascicles and/or across the fascicles of different length along the anterior–posterior axis. The present study examines differential strain along the posterior fascicles, and the companion study (Carr et al., 2011a) reveals mechanisms maintaining relatively uniform active strain among different fascicles in the anterior and posterior parts of the muscle.

Differential strain along the fascicles in a muscle has the potential to affect many aspects of muscle function as interpreted from local strain measures or muscle modeling, including predicted force and work production. Uniform fascicle strain has often been assumed to occur (Buchanan, 1999; McGowan et al., 2006; Roberts et al., 2007; Zajac, 1989), but direct evidence is lacking in most cases. Pappas et al. found nonuniform strain along the centerline fascicles of the human biceps brachii (Pappas et al., 2002). Strains in this muscle were subsequently modeled by Blemker and Delp, who were able to replicate the major features of the *in vivo* data (Blemker and Delp, 2005). Their model suggests that features of the architecture of this pinnate muscle, including nonuniform fascicle lengths, the presence of an internal aponeurosis, and fascicle curvature were responsible for the differential strain. If they modified their muscle model by making all the fascicles parallel and uniform in length, the predicted strains along the fascicles were uniform. In a study of the semimembranosus muscle of jumping toads, Ahn et al. reported that the distal segment had a different strain from the more proximal segments (Ahn et al., 2003). In the region of the toad semimembranosus studied, the fascicles vary in length and insert on a distal aponeurosis; characteristics that Blemker at al. associated with differential strain (Blemker and Delp, 2005). Pappas et al. and Ahn et al. both hypothesized that the fibers in the muscles they studied might develop nonuniform sarcomere lengths as a result of differential strain, but direct information was not available on sarcomere lengths in the muscles (Pappas et al., 2002; Ahn et al., 2003). Thus, given the limited current information, we currently cannot predict the conditions under which the fascicles of a muscle would be expected to show differential strain along their lengths, particularly in muscles with parallel fascicles. Our study tested the overall hypothesis that the strain in the fascicles from origin to insertion is relatively uniform in a muscle with long parallel fascicles.

The goals of our study were to determine whether differential strain occurs along the long fascicles of the posterior region of the ILPO, and if differential strain is observed, to test alternate hypotheses regarding the cause of the differential strain. We hypothesized that differential strain could occur because of: (1) differences in the intensity or the timing of activation along the fascicles; or (2) differences in sarcomere length along the fascicles, such that different regions of the fascicle operated on different parts of the length–tension curve.

MATERIALS AND METHODS

Overall experimental design

Using four sonomicrometer transducers spaced along the length of the fascicles, we measured the strain in proximal, central and distal segments in posterior fascicles of the ILPO in guinea fowl. The ILPO has an anterior portion with fascicles inserting on a distal aponeurosis and increasing in length from anterior to posterior (Fig. 1). The posterior fascicles are of relatively uniform length and span from an origin on the ilium to connective tissue inserting on the patellar tendon. Previous work (Buchanan, 1999) has indicated that these fascicles have approximately three in-series fibers spanning their ~80 mm length. The timing of activation was detected by inserting EMG electrodes into each segment approximately midway between each pair of transducers. The active strain of each segment was referenced to the predicted sarcomere length–tension curve using post-mortem measurements of sarcomere lengths and sonomicrometer segment lengths recorded from muscles in rigor.

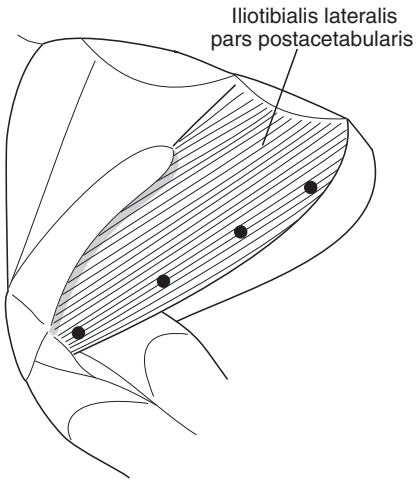

Fig. 1. Location of the iliotibialis lateralis pars postacetabularis (ILPO) in the helmeted guinea fowl thigh. Black circles indicate the position of the sonomicrometry crystals. At least one electromyographic (EMG) electrode was inserted into each segment approximately midway between each pair of transducers. Drawing by Dr David Ellerby.

Animals and training

Five guinea fowl averaging 1.54±0.08 kg body mass were used for this experiment. The guinea fowl were housed at the Northeastern University Animal Care Facility in individual cages on a 10 h:14 h light:dark cycle, with food and water provided *ad libitum*. Before surgery and experimental recordings, the birds were trained to run inside a three-sided box on a motorized treadmill. The birds were trained for 3–5 days per week for a minimum of 5 weeks. Each training session lasted 30 min. Once trained the birds could, in an individual session, maintain level speeds of 2.5 m s^{-1} for 15 min, 2.78 m s^{-1} for 3 min and 3.0 m s^{-1} for 3 min. When a bird was sufficiently trained, surgery was performed to insert sonomicrometry and EMG sensors as described below. After surgery, birds were allowed to recover in individual cages for at least 40 h before any experimental recordings. After recovery, birds were run on the treadmill and experimental recordings were taken as described below. Birds were run at speeds of 0.5, 1.0, 1.5, 2.0, 2.5, 2.78 and 3.0 m s^{-1} on a level treadmill for at least 30 s per speed. All procedures involving work with live animals were approved by the Northeastern University Animal Care and Use Committee. Animals were killed with 150 mg kg^{-1} Euthasol® (pentobarbital and phenytoin).

Muscle architecture

The ILPO covers the lateral caudal surface of the thigh. It originates on the dorsolateral iliac crest, the terminal iliac process and the posterior ischium; it inserts onto the patella, its tendon and the knee joint capsule (Fig. 1) (Gatesy, 1999). We chose to implant our sonomicrometer transducers between the long parallel fascicles in the posterior portion of the muscle because these fascicles insert close to the knee joint and have much less in-series elastic tissue than the anterior fascicles. The posterior fascicles, between which the transducers were implanted, were 82.6±3.4 mm (mean ± s.e.m.) long. The four implanted transducers spanned 73.2±3.1% of the total fascicle length.

Surgery

All transducers were sterilized (12 h ethylene oxide treatment) and implanted using sterile surgical techniques under general anesthesia

(isofluorane). Sonomicrometry transducers were made from piezoelectric transducer (PZT) discs (Boston Piezo-Optics, Inc., Bellingham, MA, USA) that were attached to 40 gauge wire, encapsulated with epoxy, and attached to stainless steel holders (Olson and Marsh, 1998). Four of these transducers were implanted between posterior fascicles of the ILPO, thus dividing the fascicles into proximal, central and distal segments (Fig. 1). Small punctures, approximately 1 mm in length, were created in the connective tissue overlying the muscle and a small, blunt probe was inserted between the fascicles to a depth of approximately 3 mm. The transducers were then placed between the fascicles. The holders were secured to the overlying connective tissue using 6-0 silk sutures. For each individual bird care was taken to ensure that the four transducers were implanted between the same fascicles along the length of the muscle.

Two fine-wire bipolar EMG electrodes were implanted into each segment of the fascicles to measure muscle activity. The electrodes were constructed from 3T stainless steel Teflon®-coated wire (Medwire, Mt Vernon, NY, USA) that was twisted coarsely along its length and more tightly near the tips. The free ends were offset with bare active tips of 1.5 mm spaced 3 mm apart. The EMG electrodes were implanted in the ILPO with a chamfered 25 gauge needle with the leads parallel to the fascicles at positions that were immediately anterior and posterior to each segment. Post-mortem examination of the implanted limb verified the placement of the sonomicrometry transducers and EMG electrodes.

Signal processing

Sonomicrometry signals were acquired digitally with a sampling frequency of 613 Hz using Sonoview software and a Sonometrics TRX Series 8 interface (Sonometrics Corp., London, ON, Canada). Digital signals were transferred to the application IGOR Pro (Wavemetrics, Inc., Portland, OR, USA) and random outliers and level shifts were corrected with custom-written functions.

The EMG signals were amplified by WPI model DAM-50 preamplifiers (World Precision Instruments, Sarasota, FL, USA) with analog high- and low-pass filters set at 10 and 3000 Hz, respectively. The amplified and filtered signals were collected at a frequency of 10 kHz using an ADInstruments Power Lab 16 bit A-D converter (Model 16SP, ADInstruments, Colorado Springs, CO, USA) controlled by a Macintosh PowerMac G4 computer (Apple, Cupertino, CA, USA) using the application Chart from ADInstruments. The EMG data were subsequently analyzed using the application IGOR Pro (Wavemetrics, Portland, OR, USA). The signals were first filtered using a finite impulse response filter with a band pass of 90–1000 Hz.

The start time, stop time and duration of the EMG bursts were all measured by manually identifying the start and end of the burst. The signal was then rectified and the average values were expressed in two ways: the average EMG amplitude per burst (equal to the integrated value for the burst divided by the burst duration); and the average EMG amplitude per stride (equal to the integrated value for the burst divided by the stride duration).

Standardization of EMG amplitude

Because significant variation exists in the EMG amplitude recorded by individual electrodes, these values are often standardized by dividing the raw values by the amplitude measured in a standard condition. However, if this standardization is done with a condition within the study it results in unequal variance across the treatment groups. Therefore, we calculated standardized EMG amplitudes by dividing by a value not reported in this study. As a standard condition we choose the value recorded from the same electrode when the animal ran up a 10% slope at 2 m s^{-1} (Carr et al., 2011b).

Videography

Videos were recorded to obtain stride timing using a NAC HV-1000 high-speed video camera (NAC Image Technology, Simi Valley, CA, USA) that recorded to VHS tape at 500 fields s^{-1}. We synchronized the EMG and sonomicrometry traces with the high-speed video recordings using a square-wave generated by the EMG recording system that was recorded at the edge of the video fields with a NAC wave inserter. Identification of foot-down and toe-off was aided by white reflective markers placed on the interphalangeal joint and the distal end of digit III.

Data were collected for ten constant-speed strides at each speed for each bird. The strides were analyzed for changes in muscle strain, muscle velocity and electrical activity.

Myofilament length and predicted sarcomere length–tension curve

An idealized sarcomere length–tension curve for the guinea fowl ILPO was estimated using the myofilament lengths from the ILPO and applying estimates based on previous single-fiber length–tension curves. The length of two thin filaments plus the *z*-line has been estimated to be 2.26 μm [corrected from data in Buchanan (Buchanan, 1999)]. This measurement of thin filament length is similar to that found in the domestic fowl (Littlefield and Fowler, 2002). Thick filament length in the ILPO of guinea fowl was taken to be 1.6 μm (Buchanan, 1999), a value consistent with most measurements of vertebrate skeletal muscle thick filaments (Gordon et al., 1966a; Gordon et al., 1966b; Littlefield and Fowler, 2002). Assuming a bare zone length on the thick filament of 0.2 μm, the plateau region of the length–tension curve was calculated to span 2.26–2.46 μm. The upper end of the descending limb would occur at a length of 3.86 μm, where there is no longer any overlap of the thick and thin filaments. In addition, we assumed that the shallow ascending limb transitions to the steep ascending limb at a length of 1.6 μm, the point at which the thick filaments would contact the *z*-line. Published data indicate that the point at which the steep ascending limb falls to zero does not correspond precisely to any of the landmarks based on filament lengths (Gordon et al., 1966a; Gordon et al., 1966b). However, Gordon et al. found that the steep ascending limb fell to zero at a value that was approximately 60% of the length at the middle of the plateau region of the length–tension curve (L_0) (Gordon et al., 1966b). Based on this finding, we assume that the steep ascending limb reaches zero at 1.39 μm.

Sarcomere measurements

To convert the *in vivo* sonomicrometer measurements into sarcomere lengths, a correspondence between a particular reference sonomicrometer length ($L_{so,ref}$) and a reference sarcomere length ($L_{sc,ref}$) is needed. We obtained these reference values using muscles in rigor. After the experimental recordings of each animal were completed, the animal was killed and the pelvis and instrumented leg were immobilized to fix hip and knee joints at angles that maintained the ILPO within the normal length range found *in vivo*. The limb was allowed to sit immobilized for 6 h until the leg muscles were in full rigor. (Note that the exact joint angles obtained in rigor do not matter for this technique, just that the muscle is not forced into an extremely shortened position during the rigor process.) Once the fixed limb was in rigor $L_{so,ref}$ was recorded. In addition, muscle temperature was measured to correct for temperature effects on the speed of sound. Two

samples of the ILPO tissue, each measuring ~1 cm^3, were removed from between each crystal pair. These muscle samples were frozen using isopentane chilled in liquid nitrogen, and then sectioned longitudinally using a cryostat. To avoid fiber compression, blocks were positioned with the knife edge parallel to the long axis of the fibers. For each muscle sample, at least ten sections were placed on slides and stained using Weigert Iron Hematoxylin (Humason, 1979). At least three fibers from each slide (containing one stained section) were photographed at 1000× magnification with an Olympus DIH032861 camera (Olympus America Inc., Center Valley, PA, USA) at a resolution of 13.48 pixels μm^{-1}. Sarcomere lengths were measured using ImageJ (version 1.38, Wayne Rasband, US National Institutes of Health, http://rsb.info.nih.gov/nih-image/). In ImageJ, the length of at least ten sarcomeres in series from each fiber was measured, and the average $L_{sc,ref}$ was calculated by dividing the total length of the in-series sarcomeres by the number of sarcomeres in series. Using the reference sonomicrometer and sarcomere lengths, *in vivo* sonomicrometry lengths (L_{so}) were converted to estimated *in vivo* sarcomere lengths (L_{sc}) using the equation:

$$L_{sc} = (L_{sc,ref} / L_{so,ref}) \times L_{so} . \quad (1)$$

Length measurements are either reported in micometers, or are converted to % L_0 using the following equation:

$$\% L_0 = (L_{sc} / 2.36) \times 100 , \quad (2)$$

where L_{sc} is the calculated sarcomere length from Eqn 1, and 2.36 µm is the estimated sarcomere length in the middle of the plateau of maximum force of the calculated length–tension curve.

Length and velocity changes

Muscle lengths were measured from the sonomicrometry traces after the sonomicrometer segment lengths (in millimeters) had been converted to sarcomere lengths (in micrometers). In each stride there were two minima and two maxima in the length trajectory of the ILPO (Fig. 2). The length values measured were: $L_{min,fd}$, the minimum length of the ILPO that occurred near the time of foot-down; $L_{max,st}$, the maximum length of the ILPO occurring during stance; $L_{min,to}$, minimum length of the ILPO that occurred near the time of toe-off; $L_{max,sw}$, maximum length of the ILPO occurring during swing; L_{on}, length of the ILPO 25 ms after the start of the EMG activity; and L_{off}, length of the ILPO 25 ms after the stop of the EMG activity.

These measured lengths were used to calculate active lengthening, active shortening, passive lengthening and passive shortening. As indicated by our definitions of L_{on} and L_{off}, we assumed an electromechanical delay of 25 ms when we calculated active shortening and active lengthening. We are not aware of studies done on the ILPO to confirm this assumption, but this time period falls within values measured for other muscles (Cavanagh and Komi, 1979; Moritani et al., 1987; Winter and Brookes, 1991; Zhou et al., 1995; Gabriel and Boucher, 1998; Muraoka et al., 2004; Roberts and Gabaldon, 2008). The equation used to calculate a given length change was dependent on the timing of L_{on} and L_{off} relative to other lengths measured during a stride. Active lengthening (ΔL_{al}) was calculated using one of two equations. If L_{on} occurred before $L_{min,fd}$ then:

$$\Delta L_{al} = L_{max,st} - L_{min,fd} . \quad (3)$$

If L_{on} occurred after $L_{min,fd}$ then:

$$\Delta L_{al} = L_{max,st} - L_{on} . \quad (4)$$

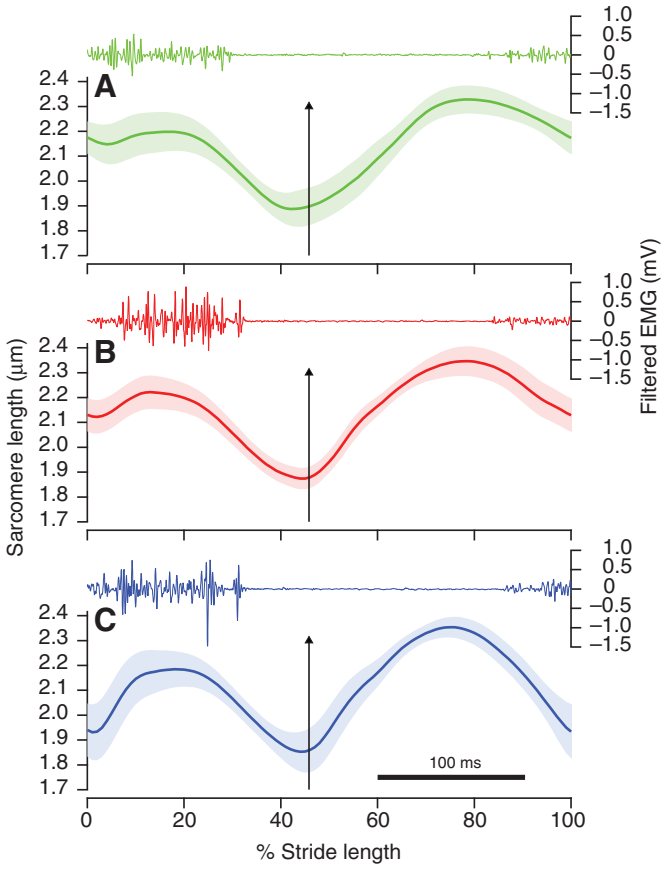

Fig. 2. The mean proximal (green, A), central (red, B) and distal (blue, C) sarcomere lengths of the ILPO posterior fascicles of the guinea fowl running at 2.5 m s^{-1} for one stride. Time axis is expressed as a percentage of the stride duration from foot-down to foot-down. The black bar in C indicates 100 ms. The black arrow indicates toe-off. The shaded areas represent ±1 s.e.m. One representative filtered EMG trace is also shown for each segment.

Active shortening (ΔL_{as}) was calculated using one of two equations. If L_{off} occurred after $L_{min,to}$ then:

$$\Delta L_{as} = L_{max,st} - L_{min,to} . \quad (5)$$

If L_{off} occurred before $L_{min,to}$ then:

$$\Delta L_{as} = L_{max,st} - L_{off} . \quad (6)$$

Passive lengthening (ΔL_{pl}) was calculated using one of two equations. If L_{off} occurred before $L_{min,to}$ then:

$$\Delta L_{pl} = L_{max,sw} - L_{min,to} . \quad (7)$$

If L_{off} occurred after $L_{min,to}$ then:

$$\Delta L_{pl} = L_{max,sw} - L_{off} . \quad (8)$$

Passive shortening (ΔL_{ps}) was calculated using one of two equations. If L_{on} occurred after $L_{min,fd}$ then:

$$\Delta L_{ps} = L_{max,sw} - L_{min,fd} . \quad (9)$$

If L_{on} occurred before $L_{min,fd}$ then:

$$\Delta L_{ps} = L_{max,sw} - L_{on} . \quad (10)$$

All length changes are reported as % L_0 where L_0 is equal to 2.36 µm, the length at the middle of the plateau region of the length–tension curve.

Table 1. Results of the ANOVA model for active and passive strain and active velocity of segments of the posterior fascicles of the iliotibialis lateralis pars postacetabularis (ILPO)

		Active strain				Passive strain				Active velocity			
		Shortening		Lengthening		Lengthening		Shortening		Lengthening		Shortening	
Effect	d.f.	*F*	*P*	*F*	*P*	*F*	*P*	*F*	*P*	*F*	*P*	*F*	*P*
Bird ID[a]	4,92	7.972	**<0.001**	48.18	**<0.001**	5.616	**<0.001**	7.629	**<0.001**	3.657	**0.008**	9.386	**<0.001**
Speed[b]	6,92	1.1636	0.146	33.169	**<0.001**	14.968	**<0.001**	1.014	0.421	28.78	**<0.001**	67.325	**<0.001**
Segment[c]	2,92	41.596	**<0.001**	0.215	0.807	5.485	**0.006**	32.241	**<0.001**	60.18	**<0.001**	3.006	0.054

Significant *P*-values are shown in bold type.
[a]Identifier for the individual birds entered as a random factor.
[b]Treadmill speed entered as a fixed factor.
[c]Segment position (proximal, central, distal) entered as a fixed factor.

Table 2. *Post hoc* paired comparisons of active and passive strain and velocity at different positions (proximal, central and distal) along the posterior fascicles of the ILPO

		Active strain				Passive strain				Active velocity			
		Shortening		Lengthening		Lengthening		Shortening		Lengthening		Shortening	
Effect	d.f.	*F*	*P*	*F*	*P*	*F*	*P*	*F*	*P*	*F*	*P*	*F*	*P*
Segment	Proximal	Central	Proximal	Central	Proximal	Central	Proximal	Central	Proximal	Central	Proximal	Central	
Proximal	–	>0.999	–	*	–	0.167	–	0.343	–	**0.029**	–	*	
Distal	**<0.001**	**<0.001**	*	*	**0.004**	0.533	**<0.001**	**<0.001**	**<0.001**	**<0.001**	*	*	

Values shown are *P*-values for the paired comparison with the Bonferroni correction applied.
*No significant effect of segment position in the overall model.

Average velocities were calculated during active lengthening and shortening and in each compartment and speed. Average velocities, in lengths per second, were calculated by dividing the amount of active lengthening or active shortening (expressed as a fraction of L_0) by the duration of lengthening or shortening. Thus the average velocity during active lengthening (V_{al}) is:

$$V_{al} = \Delta L_{al} / (2.36 \times t_{al}), \quad (11)$$

where ΔL_{al} is the active lengthening from Eqn 3 or 4, 2.36 μm is the length at the center of the plateau region of the length–tension curve and t_{al} is the duration of active lengthening in seconds.

Similarly, the velocity during active shortening (V_{as}) is:

$$V_{as} = \Delta L_{as} / (2.36 \times t_{as}), \quad (12)$$

where ΔL_{as} is the active shortening from Eqn 5 or 6, 2.36 μm is the length at the center of the plateau region of the length–tension curve and t_{as} is the duration of active shortening in seconds.

Statistical analysis

ANOVA was conducted using the general linear model in the application SPSS (version 18.0 for Mac OS, SPSS Inc., Chicago, IL, USA). In addition to the dependent variables, the ANOVA models included the following effects: animal identifier as a random factor, segment position (proximal, central and distal) as a fixed factor and speed as a fixed factor. If the ANOVA model showed a significant effect of segment position, *post hoc* paired comparisons among the different segments were performed using a Bonferroni correction. Results of all statistical tests were considered significant if the *P*-values were less than 0.05. Results are reported as means ± 1 standard error of the mean (s.e.m.).

RESULTS

Strain and velocity

The proximal, central and distal (Fig. 2A–C) segments of the posterior ILPO showed the same general pattern of lengthening and activation during running. Electrical activity in the posterior ILPO started in late swing and proceeded through most of the stance phase. During the stance phase, the posterior ILPO was initially lengthened while active, and then shortened actively in the latter half of the stance. During the swing phase, when the muscle is inactive, it was passively lengthened and then passively shortened.

Although the general pattern of strain was similar in all the segments of the posterior ILPO, significant quantitative differences were found among the segments after accounting for the significant effects of locomotor speed and variation among the individual birds (Tables 1 and 2). During the active part of the cycle the distal segment was lengthened significantly more than the central or proximal segments (Fig. 3A). However, during the subsequent shortening the differences in strain among the segments were not significant. The differences in strain among the segments was also reflected in the velocities, with a gradient of increasing velocity from proximal to distal during active lengthening and no significant differences among the segments during active shortening (Fig. 4). During swing phase when the muscle was passive, we found significantly larger strain in the distal segment during both lengthening and shortening (Fig. 3B). The difference in passive strain was smaller during passive lengthening than that found during passive shortening. The strains in the distal segment during passive shortening were approximately twice those found in the proximal segment.

Predicted sarcomere operating lengths

On the basis of our calculated length–tension curves, active lengthening of all the segments of the fascicles in the posterior ILPO occurred on the shallow ascending limb of the curve (Fig. 5). After accounting for significant variation among the individuals (the speed effect was not significant) we found significant effects of segment position on the sarcomere lengths during the active part of the stride (Table 3). The largest difference among the segments was in the length at the beginning of active lengthening ($L_{min,fd}$), the value of which was significantly shorter than those

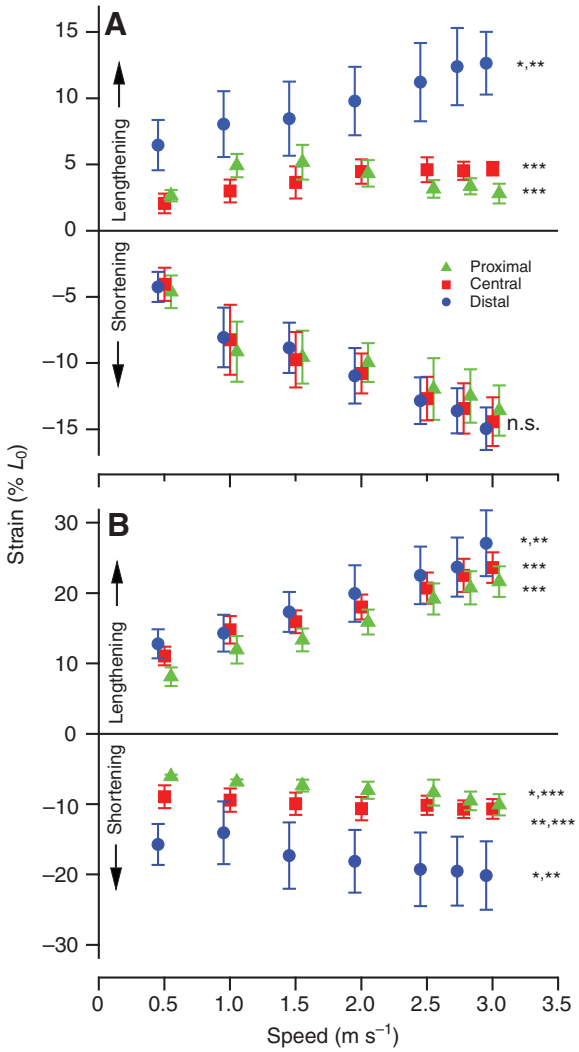

Fig. 3. Active (A) and passive (B) strains in the proximal (green triangles), central (red squares) and distal (blue circles) portions of the posterior ILPO. If the paired comparisons (Table 2) demonstrated a significant difference because of position, the results were classified as: significantly different from proximal (*); significantly different from central (**); significantly different from distal (***); or not significant (n.s.). We designated shortening strain as positive and lengthening as negative. Proximal and distal values are offset slightly on the speed axis for clarity. Error bars indicate ±1 s.e.m.

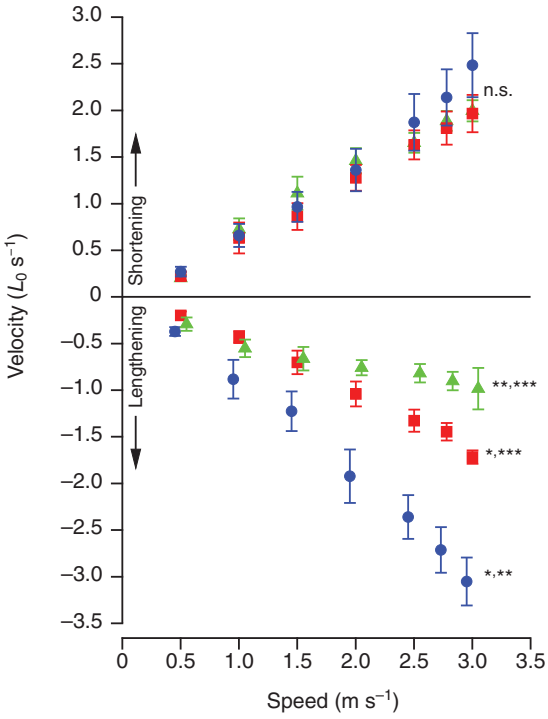

Fig. 4. Average velocity during active lengthening and active shortening in the proximal (green triangles), central (red squares) and distal (blue circles) portions of the posterior ILPO. We designated shortening velocity as positive and lengthening as negative. If the paired comparisons (Table 2) demonstrated a significant difference due to position, the results were classified as: significantly different from proximal (*); significantly different from central (**); significantly different from distal (***); or not significant (n.s.). Proximal and distal results are are offset slightly on the speed axis for clarity. Error bars indicate ±1 s.e.m.

for the proximal or central segments (paired comparison, $P<0.001$). This result correlates with the larger strain found during active lengthening of this segment. We also found a significant effect ($P=0.032$) of segment position on the maximum sarcomere length in stance after active lengthening ($L_{max,st}$). However, in paired comparisons this difference was revealed to be due to a small difference between proximal and central values ($P=0.03$), and most of the variance in this value was explained by variation among birds (Table 3).

Electromyography

After accounting for the large effect of speed and of variation among individuals, none of the measures of standardized EMG amplitude or timing showed significant effects of segment position (Figs 6 and 7; Table 4).

DISCUSSION

Our results demonstrate that all parts of the long posterior fascicles of the ILPO underwent lengthening followed by shortening, both while active in stance phase and when inactive during swing phase. However, significant quantitative differences in strain occurred along the length of the fascicles during active lengthening, passive shortening and passive lengthening (Fig. 3). The magnitude of strain occurring during these phases of the strain cycle was always much greater in the distal portion of the fascicle than it was in the proximal and central portions. These data refute the overall hypothesis that the strain cycle during the period of muscle activity is quantitatively similar along the fascicle. During the time when the ILPO is being lengthened while active, the distal portion lengthens significantly more than either the proximal or central portion of the muscle.

Alternative hypotheses to explain differential active lengthening along the fascicles

We tested two alternative hypotheses regarding the cause of the larger strain in the more distal segment during active lengthening of the long posterior fascicles of the ILPO. First, we considered the hypothesis that the distal fascicles show delayed or reduced activation. Buchanan found that the long posterior fascicles of the ILPO are spanned by three overlapping in-series fibers, and therefore differences in activation timing are possible if the proximal and distal fibers are innervated by different motor neurons (Buchanan, 1999). We do not know the motor unit organization of the in-series fibers

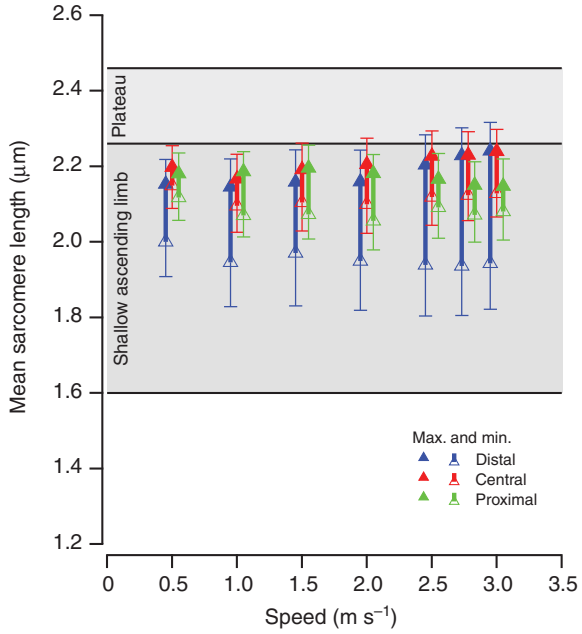

Fig. 5. Starting (open symbols) and ending (closed symbols) sarcomere lengths during active lengthening as a function of speed in the proximal (green), central (red) and distal (blue) portions of the posterior ILPO. Thick solid bars connect the start (minimum) and end (maximum) lengths for each segment. Error bars indicate –1 s.e.m. for the start length and +1 s.e.m. for the end length. Shaded areas indicate the calculated plateau and ascending limb of guinea fowl ILPO length–tension curve, based on filament lengths.

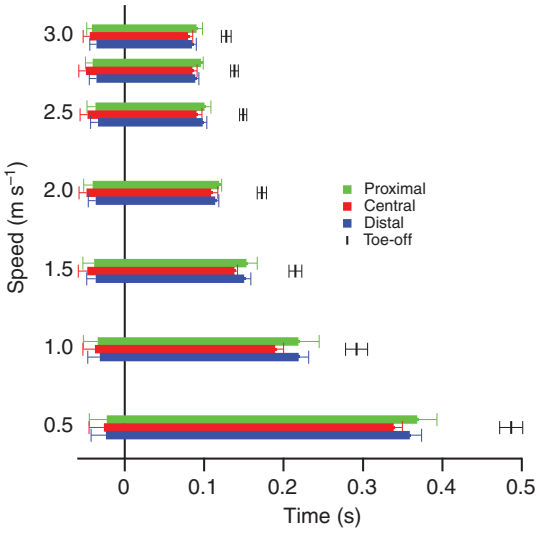

Fig. 6. EMG start and stop times relative to foot-down in the proximal (green bars), central (red bars) and distal (blue bars) portions of the posterior ILPO at speeds between 0.5 and 3.0 m s^{-1}. Zero time indicates foot-down. Solid horizontal bars extend from the mean EMG start to the mean EMG end. Vertical bars with error bars indicate mean stance duration ± 1 s.e.m. Error bars indicate –1 s.e.m. for the start time and +1 s.e.m. for the end time.

in the ILPO, but data from pigeon pectoralis (Sokoloff et al., 1998) suggest that avian in-series fibers can be innervated by separate motor units. If the distal segments of the ILPO fascicles have reduced or delayed activation compared with more proximal segments, they would have reduced maximum force-generating capacity and would lengthen more when the knee flexes in early stance. Differential activation of fascicles operating in parallel within a single muscle has been demonstrated in other muscles in guinea fowl and cats (Chanaud et al., 1991; Higham and Biewener, 2008; Higham et al., 2008; Hoogendyk et al., 2005). However, differential activation along fascicles with in-series fibers has been generally considered to be undesirable, because it would compromise effective force transmission. To allow for effective force generation and avoid overstretching passive portions of the fascicle, nearly simultaneous activation is predicted. Thus, perhaps not surprisingly, our data contradicted the hypothesis of differential activation as an explanation for the differential lengthening of the active segments of the ILPO. The timing was similar in all segments as were all our quantitative measures of the amount of activation (Figs 6 and 7).

The second hypothesis we tested that might explain the larger active lengthening in the distal segment is that the sarcomeres in this region begin activity at a shorter sarcomere length. If the sarcomeres in the distal segment start activity lower on the ascending limb of the length–tension curve, they would have reduced force-producing capacity despite having similar activation. Our data on sarcomere lengths are consistent with this and could account for the differential strain. The distal segment began active lengthening when the sarcomeres in this region had significantly shorter mean sarcomere lengths (Fig. 5) compared with the more proximal segments. By the end of active stretch, the sarcomeres in all segments were lengthened to approximately the same length, and because the active strains during shortening were similar in all segments (Fig. 3), the sarcomeres ended shortening at similar lengths on the calculated sarcomere length–tension curve (Fig. 5).

Table 3. Results of the ANOVA model for sarcomere lengths of segments of the posterior fascicles of the ILPO

		Sarcomere lengths					
		$L_{min,fd}$		$L_{max,st}$		$L_{min,to}$	
Effect	d.f.	*F*	*P*	*F*	*P*	*F*	*P*
Bird ID[a]	4,92	71.229	**<0.001**	128.704	**<0.001**	41.094	**<0.001**
Speed[b]	6,92	0.515	0.795	1.149	0.341	23.155	**<0.001**
Segment[c]	2,92	26.672	**<0.001**	3.589	**0.031**	2.411	0.095

Significant *P*-values are shown in bold type.
[a]Identifier for the individual birds entered as a random factor.
[b]Treadmill speed entered as a fixed factor.
[c]Segment position (proximal, central, distal) entered as a fixed factor.
$L_{max,st}$, maximum length of the ILPO occurring during stance; $L_{min,fd}$, minimum length of the ILPO that occurred near the time of foot down; $L_{min,to}$, minimum length of the ILPO that occurred near the time of toe-off.

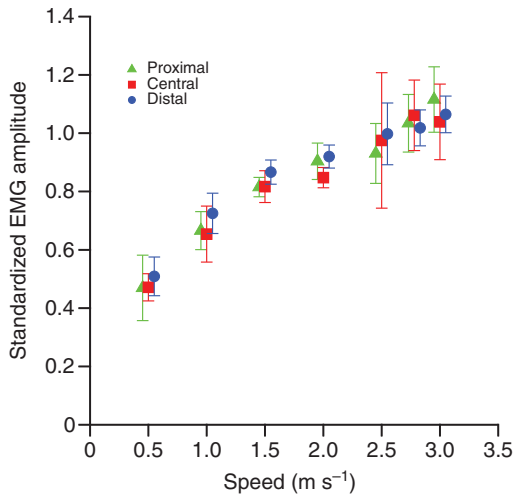

Fig. 7. Standardized average EMG amplitude per stride as a function of speed for the proximal (green triangles), central (red squares) and distal (blue circles) portions of the posterior ILPO. Error bars indicate ±1 s.e.m.

All the stretch of the ILPO occurs on the ascending limb of the predicted length–tension curve (Fig. 7). Sarcomere lengths within a muscle fiber (or fascicle) are considered to be self-stabilizing when stretched while active on the ascending limb (Morgan, 1990). Although Morgan modeled the effects of random heterogeneity in strength at the same sarcomere length or random variation in sarcomere length along the fiber, the same principles should apply to systematic variation in sarcomere length along the fiber (Morgan, 1990). Self-stabilization occurs because the weaker sarcomeres become stronger as they are lengthened on the ascending limb. Note that the actual force along the sarcomeres in series is expected to be the same; the differences among the sarcomeres are in their maximum force-generating capacities. Sarcomeres with different maximum force-generating capacities will have different behavior when the same force is applied as a result of force–velocity effects. Shorter, weaker sarcomeres will lengthen under the same force that longer, stronger sarcomeres can support isometrically. In the ILPO the average sarcomere length at the beginning of active lengthening was significantly shorter in the distal segment, and during lengthening these distal sarcomeres reached approximately the same mean length as the more proximal sarcomeres, which is consistent with the hypothesis of self-stabilization on the ascending limb.

Beyond the match of the second hypothesis with the predicted steady-state force–length properties of skeletal muscle, our data are also consistent with what is known about the transient effects of active lengthening. Many studies of active lengthening are difficult to apply precisely to our data because the experimental conditions differ from those found for the ILPO. Typical studies of active lengthening lengthen fully active muscles or single above the optimal sarcomere length (Flitney and Hirst, 1978; Edman et al., 1978; Cavagna et al., 1981; Cavagna et al., 1986; Sugi and Tsuchiya, 1981; Takarada et al., 1997). We know of no study that has examined lengthening of muscle fibers under conditions similar to those we have described for the ILPO, i.e. fibers starting at different values of L/L_0 on the ascending limb of the isometric length–tension curve, subjected to the same force at these different lengths, and lengthening starting shortly after the onset of stimulation. However, several studies have examined conditions mimicking one or more of these conditions. Faster lengthening of the distal segment is consistent with data in Joyce and Rack showing that, subjected to the same level of isotonic force, cat soleus lengthens faster and by a larger amount when lengthening starts at a shorter length (Joyce and Rack, 1969). This more rapid lengthening is consistent with the force-generating capacity of the fibers being lower during the lengthening transient when lengthening starts at shorter lengths (Edman et al., 1978). The different segments of the ILPO show similar amounts of shortening after being lengthened by differing amounts and differing velocities. These data are consistent with the potentiating after effects of lengthening being reduced or absent when, as in the ILPO, stretch occurs on the ascending limb (Edman et al., 1978; Ettema et al., 1990). In the future it may be possible to model the effects seen in the ILPO, but such a model would also have to incorporate the effects of stimulation (Joyce and Rack, 1969; Joyce et al., 1969).

The cause of the differential strain that we note in this study appears to be different from those suggested previously in work on the biceps brachii of humans (Pappas et al., 2002; Blemker and Delp, 2005) and semitendinosus of toads (Ahn et al., 2003). These studies focused on architectural features of the muscle (including the presence of an internal aponeurosis) as the possible reasons of differences in active strain, and considered non-uniform sarcomere length as a result of the differential active strain. The model of Blemker and Delp was able to predict non-uniform strains when all the sarcomeres started at the same length (Blemker and Delp, 2005).

What mechanisms result in the distal segment beginning activity at shorter sarcomere lengths?

Our data indicate that passive length changes occurring between the end of one active period and the beginning of the next are important in determining the starting sarcomere lengths when activity begins. Thus, the differences in active lengthening are predicted to result from events occurring in the passive part of the

Table 4. Results of the ANOVA model for variables related to the electromyographic (EMG) activity of segments of the posterior fascicles of the ILPO

		Standardized average EMG amplitude									
		Per burst		Per stride		Start time		Stop time		Duration	
Effect	d.f.	*F*	*P*	*F*	*P*	*F*	*P*	*F*	*P*	*F*	*P*
Bird ID[a]	4,92	26.01	**<0.001**	8.78	**<0.001**	27.50	**<0.001**	14.131	**<0.001**	13.847	**<0.001**
Speed[b]	6,92	43.48	**<0.001**	29.20	**<0.001**	2.274	**0.047**	544.653	**<0.001**	142.595	**<0.001**
Segment[c]	2,92	0.832	0.444	0.178	0.838	2.645	0.079	0.167	0.847	0.496	0.611

Significant *P*-values are shown in bold type.
[a]Identifier for the individual birds entered as a random factor.
[b]Treadmill speed entered as a fixed factor.
[c]Segment position (proximal, central, distal) entered as a fixed factor.

length cycle. The problem with presenting a precise hypothesis about the determinants of differential strain when the muscle is passive is that the determinants of the passive length changes are probably complex and estimates of fascicle length changed by sonomicrometry (or other methods) may not necessarily accurately reflect local sarcomere length change in a slack muscle. An isolated muscle being passively deformed by forces applied only at the proximal and distal ends could be modeled, given sufficient knowledge of its passive visco-elastic properties and slack length. However, for a passive muscle embedded among muscles and other structures in the limb, significant lateral and shear forces are probably applied by surrounding active and passive muscles, and it is quite possible that these forces are large enough to cause differential passive strain within the muscle.

Consequences of non-uniform strain for studies of muscle function using local strain measurements

Because of signal strength issues, sonomicrometry is typically limited to fascicle segments of 25 mm or less. Thus, if the goal is to assess the overall strain cycle of muscles with long fascicles, non-uniform strain becomes an important issue to consider: given strain differences along the fascicle, quantitatively accurate strain can only be determined by measurements along most of the length of the fascicle. For the ILPO the local strain measurements in the posterior fascicles all have the same qualitative shape but differ in the amount of active lengthening. Data in another guinea fowl muscle, the iliofibularis (Hoogendyk et al., 2005) (T. Hoogendyk, personal communication), indicate that in some muscles with long parallel fascicles, measurements of a single segment do reflect the overall strain. Intriguingly, the iliofibularis undergoes little active lengthening, and this may indicate that differential strain is associated with active lengthening. Shortening fibers are expected to rapidly stabilize sarcomere length because of the inverse relationship between force and velocity on the shortening portion of the force–velocity curve.

Conclusions

We rejected the hypothesis that active strain is similar along the long posterior fascicles of the ILPO muscle in guinea fowl during walking and running because, although strain during active shortening was similar in all segments of the fascicle, the distal segment of the fascicle lengthened to a greater extent when active than did the more proximal segments. The larger amount of active lengthening in the distal segment was not caused by differential activation. Instead our data support the hypothesis that the distal segment lengthened farther and faster because it began activity at shorter sarcomere lengths on the ascending limb of the length–tension curve. Owing to the self-stabilizing effects of operating on the ascending limb, the segments reached the end of lengthening and started shortening at approximately the same sarcomere length. During shortening this similarity in sarcomere length among the segments is maintained, as predicted from force–velocity effects. The differential active strain during lengthening is thus determined by differences in strain during the passive portion of the cycle. All segments of the fascicles were at similar sarcomere lengths at the end of active shortening, but after the passive portion of the cycle, the distal segment was shorter. Differential strain in the segments during the passive portion of the cycle may be caused by differential joint excursions at the knee and hip acting on the ends of the muscle and being transmitted differentially by the bulk passive visco-elastic properties of the muscle. Alternatively, the differential passive strain could also be determined by the transmission of shear forces from the surrounding muscles and other structures in the thigh. On the basis of basic sarcomere dynamics we suggest that differential strain is more likely in muscles undergoing active lengthening at the beginning of contraction than those undergoing only shortening.

LIST OF SYMBOLS AND ABBREVIATIONS

ILPO	iliotibialis lateralis pars postacetabularis
L_0	the length at the middle of the plateau region of the length–tension curve (optimal length)
$L_{max,st}$	maximum length of the ILPO occurring during stance
$L_{max,sw}$	maximum length of the ILPO occurring during swing
$L_{min,fd}$	minimum length of the ILPO that occurred near the time of foot-down
$L_{min,to}$	minimum length of the ILPO that occurred near the time of toe-off
L_{off}	length of the ILPO 25 ms after the stop of the EMG activity
L_{on}	length of the ILPO 25 ms after the start of the EMG activity
L_{sc}	*in vivo* sarcomere lengths
$L_{sc,ref}$	reference sarcomere length
L_{so}	*in vivo* segment lengths measured by sonomicrometry
$L_{so,ref}$	sonomicrometer length
t_{al}	duration of active lengthening
V_{al}	average velocity during active lengthening
V_{as}	velocity during active shortening
ΔL	passive shortening
ΔL_{al}	active lengthening
ΔL_{as}	active shortening
ΔL_{as}	active shortening
ΔL_{pl}	passive lengthening

ACKNOWLEDGEMENTS

This work was supported by grants NIH RO1-AR47337 and NSF IOB-0542795 to R.L.M. Jade McPherson, Havalee Henry, Thomas Hoogendyk, Karen Bioski, Francis Carr and Julia Vasic helped with the *in vivo* experiments and data analysis. We also thank Drs Gwilym Jones, Rebecca Rosengaus and Frederick Davis for helpful suggestions during the course of the research and for comments on a draft of this work that formed a portion of J.A.C.'s PhD dissertation. Deposited in PMC for release after 12 months.

REFERENCES

Ahn, A. N., Monti, R. J. and Biewener, A. A. (2003). In vivo and in vitro heterogeneity of segment length changes in the semimembranosus muscle of the toad. *J. Physiol.* **549**, 877-888.

Blemker, S. S. and Delp, S. L. (2005). Three-dimensional representation of complex muscle architectures and geometries. *Ann. Biomed. Eng.* **33**, 661-673.

Buchanan, C. I. (1999). *Muscle Function and Tendon Adaptation in Guinea Fowl (*Numida meleagris*)*. PhD thesis, 131 pp., Northeastern University, Boston, MA, USA.

Carr, J. A., Ellerby, D. J., Rubenson, J. and Marsh, R. L. (2011a). Mechanisms producing coordinated function across the breadth of a large biarticular thigh muscle. *J. Exp. Biol.* **214**, 3396-3404.

Carr, J. A., Ellerby, D. J. and Marsh, R. L. (2011b). Function of a large biarticular hip and knee extensor during walking and running in guinea fowl (*Numida meleagris*). *J. Exp. Biol.* **214**, 3405-3413.

Cavagna, G. A., Citterio, G. and Jacini, P. (1981). Effects of speed and extent of stretching on the elastic properties of active frog muscle. *J. Exp. Biol.* **91**, 131-143.

Cavagna, G. A., Mazzanti, M., Heglund, N. C. and Citterio, G. (1986). Mechanical transients intitiated by ramp stretch and release to P0 in frog muscle fibers. *Am. J. Physiol.* **251**, C571-C579.

Cavanagh, P. R. and Komi, P. V. (1979). Electromechanical delay in human skeletal muscle under concentric and eccentric contractions. *Eur. J. Appl. Physiol. Occup. Physiol.* **42**, 159-163.

Chanaud, C. M., Pratt, C. A. and Loeb, G. E. (1991). Functionally complex muscles of the cat hindlimb. II. Mechanical and architectural heterogenity within the biceps femoris. *Exp. Brain Res.* **85**, 257-270.

Edman, K. A. P., Elzinga, G. and Noble, M. I. M. (1978). Enhancement of mechanical performance by stretch during tetanic contractions of vertebrate skeletal muscle fibres. *J. Physiol. Lond.* **281**, 139-155.

Ellerby, D. J., Henry, H. T., Carr, J. A., Buchanan, C. I. and Marsh, R. L. (2005). Blood flow in guinea fowl *Numida meleagris* as an indicator of energy expenditure by individual muscles during walking and running. *J. Physiol.* **564**, 631-648.

Ettema, G. J. C., Vansoest, A. J. and Huijing, P. A. (1990). The role of series elastic structures in prestretch-induced work enhancement during isotonic and isokinetic contractions. *J. Exp. Biol.* **154**, 121-136.

Flitney, F. W. and Hirst, D. G. (1978). Cross-bridge detachment and sarcomere 'give' during stretch of active frog's muscle. *J. Physiol.* **276**, 449-465.

Gabriel, D. A. and Boucher, J. P. (1998). Effects of repetitive dynamic contraction upon electromechanical delay. *Eur. J. Appl. Physiol. Occup. Physiol.* **79**, 37-40.
Gatesy, S. M. (1999). Guineafowl hindlimb function II: electromyographic analysis and motor pattern evolution. *J. Morphol.* **240**, 127-142.
Gordon, A. M., Huxley, A. F. and Julian, F. J. (1966a). Tension development in highly stretched vertebrate muscle fibres. *J. Physiol.* **184**, 143-169.
Gordon, A. M., Huxley, A. F. and Julian, F. J. (1966b). The variation in isometric tension with sarcomere length in vertebrate muscle fibres. *J. Physiol.* **184**, 170-192.
Higham, T. E. and Biewener, A. A. (2008). Integration within and between muscles during terrestrial locomotion: effects of incline and speed. *J. Exp. Biol.* **211**, 2303-2316.
Higham, T. E., Biewener, A. A. and Wakeling, J. M. (2008). Functional diversification within and between muscle synergists during locomotion. *Biol. Lett.* **4**, 41-44.
Hoogendyk, T., Carr, J. A., Henry, H. T., Rubenson, J. and Marsh, R. L. (2005). Mechanical and neural determinants of differences in fascicle strain between functionally distinct compartments in *M. Iliofibularis* during terrestrial locomotion in guinea fowl (*Numida meleagris*). SICB Annual Meeting, 4-8 January 2008, San Diego, CA.
Humason, G. L. (1979). *Animal Tissue Techniques*. San Francisco: W. H. Freeman and Company.
Joyce, G. C. and Rack, P. M. (1969). Isotonic lengthening and shortening movements of cat soleus muscle. *J. Physiol.* **204**, 475-491.
Joyce, G. C., Rack, P. M. and Westbury, D. R. (1969). The mechanical properties of cat soleus muscle during controlled lengthening and shortening movements. *J. Physiol.* **204**, 461-474.
Lieberman, D. E., Raichlen, D. A., Pontzer, H., Bramble, D. M. and Cutright-Smith, E. (2006). The human gluteus maximus and its role in running. *J. Exp. Biol.* **209**, 2143-2155.
Littlefield, R. and Fowler, V. M. (2002). Measurement of thin filament lengths by distributed deconvolution analysis of fluorescence images. *Biophys. J.* **82**, 2548-2564.
Marsh, R. L., Ellerby, D. J., Carr, J. A., Henry, H. T. and Buchanan, C. I. (2004). Partitioning the energetics of walking and running: swinging the limbs is expensive. *Science* **303**, 80-83.
McGowan, C. P., Duarte, H. A., Main, J. B. and Biewener, A. A. (2006). Effects of load carrying on metabolic cost and hindlimb muscle dynamics in guinea fowl (*Numida meleagris*). *J. Appl. Physiol.* **101**, 1060-1069.
Morgan, D. L. (1990). New insights into the behavior of muscle during active lengthening. *Biophys. J.* **57**, 209-221.
Moritani, T., Berry, M. J., Bacharach, D. W. and Nakamura, E. (1987). Gas exchange parameters, muscle blood flow and electromechanical properties of the plantar flexors. *Eur. J. Appl. Physiol. Occup. Physiol.* **56**, 30-37.
Muraoka, T., Muramatsu, T., Fukunaga, T. and Kanehisa, H. (2004). Influence of tendon slack on electromechanical delay in the human medial gastrocnemius in vivo. *J. Appl. Physiol.* **96**, 540-544.
Olson, J. M. and Marsh, R. L. (1998). Activation patterns and length changes in hindlimb muscles of the bullfrog *Rana catesbeiana* during jumping. *J. Exp. Biol.* **201**, 2763-2777.
Osternig, L. R., Caster, B. L. and James, C. R. (1995). Contralateral hamstring (biceps femoris) coactivation patterns and anterior cruciate ligament dysfunction. *Med. Sci. Sports Exerc.* **27**, 805-808.
Pappas, G. P., Asakawa, D. S., Delp, S. L., Zajac, F. E. and Drace, J. E. (2002). Nonuniform shortening in the biceps brachii during elbow flexion. *J. Appl. Physiol.* **92**, 2381-2389.
Roberts, T. J. and Gabaldon, A. M. (2008). Interpreting muscle function from EMG: lessons learned from direct measurements of muscle force. *Int. Comp. Biol.* **48**, 312-320.
Roberts, T. J., Higginson, B. K., Nelson, F. E. and Gabaldon, A. M. (2007). Muscle strain is modulated more with running slope than speed in wild turkey knee and hip extensors. *J. Exp. Biol.* **210**, 2510-2517.
Sokoloff, A. J., Ryan, J. M., Valerie, E., Wilson, D. S. and Goslow, G. E., Jr (1998). Neuromuscular organization of avian flight muscle: morphology and contractile properties of motor units in the pectoralis (pars thoracicus) of pigeon (*Columba livia*). *J. Morphol.* **236**, 179-208.
Sugi, H. and Tsuchiya, T. (1981). Enhancement of mechanical performance in frog muscle fibres after quick increases in load. *J. Physiol. Lond.* **319**, 239-252.
Takarada, Y., Iwamoto, H., Sugi, H., Hirano, Y. and Ishii, N. (1997). Stretch-induced enhancement of mechanical work production in frog single fibers and human muscle. *J. Appl. Physiol.* **83**, 1741-1748.
Winter, E. M. and Brookes, F. B. (1991). Electromechanical response times and muscle elasticity in men and women. *Eur. J. Appl. Physiol. Occup. Physiol.* **63**, 124-128.
Zajac, F. E. (1989). Muscle and tendon: properties, models, scaling, and application to biomechanics and motor control. *Crit. Rev. Biomed. Eng.* **17**, 359-411.
Zhou, S., Lawson, D. L., Morrison, W. E. and Fairweather, I. (1995). Electromechanical delay in isometric muscle contractions evoked by voluntary, reflex and electrical stimulation. *Eur. J. Appl. Physiol. Occup. Physiol.* **70**, 138-145.